Journal of Agricultural Engineering

Journal of Agricultural Engineering 2026; LVII:1766
doi:10.4081/jae.2025.1766

AI-powered autonomous spraying robot for precision orchard applications

Dilara Gerdan Koc,[1] Caner Koc,[1] Mustafa Comakli[2]

[1]Department of Agricultural Machinery and Technologies Engineering, Faculty of Agriculture, Ankara University, Ankara; [2]Department of Agricultural Machinery and Technologies Engineering, Faculty of Agriculture, Atatürk University, Erzurum, Turkey

Abstract

In this study, an electric and autonomous orchard spraying robot, named OrcBOT, was developed, modeled, and prototyped for precision orchard spraying. The system integrates electrostatically charged nozzles with YOLOv5-based real-time canopy detection, enabling highly precise and variable-rate pesticide application through independent nozzle control. Spraying operations are coordinated using stereo cameras and RTK-GPS navigation, while nozzle activation is managed by a central electronic control unit based on canopy structure. The robot is capable of both remote-controlled and fully autonomous operation, with monitoring and control accessible via smartphone and tablet applications. Field trials conducted in apple orchards using food dye as a tracer demonstrated an average droplet size of 150-170 µm, classified as fine spray according to ASAE S572.1. Canopy coverage averaged 55%, reaching up to 57% under optimal operating conditions (2 bar, 1 km/h, 10 kV). These findings demonstrate the effectiveness of OrcBOT in fine pulverization applications and underline its potential as a sustainable and practical solution for precision orchard spraying.

Key words: autonomous robot; AI spraying; canopy detection; deep learning; precision spraying.

Correspondence: Dilara Gerdan Koc, Department of Agricultural Machinery and Technologies Engineering, Faculty of Agriculture, Ankara University, Ankara, Turkey. E-mail: dgerdan@ankara.edu.tr

Introduction

The agricultural sector is essential for sustaining the global population, especially in rural and low-income areas. The United Nations projects that the global population will reach roughly 9.7 billion by 2050, resulting in an anticipated 50% increase in agricultural demand relative to 2012 levels (Çilingir and Dursun, 2010; United Nations, 2024). Notwithstanding this anticipated growth, it is projected that between 600 and 670 million individuals will continue to experience undernourishment by 2030 (Çilingir and Dursun, 2010), highlighting the critical necessity for technological advancements in food production. Increasing productivity per unit area has thus become a primary goal in agricultural policy, requiring advancements in precision farming, automation, and resource-efficient production to address future food security challenges.

Within these conditions, one of the most resource-intensive and environmentally critical operations in agriculture is pesticide application. Addressing inefficiencies in pesticide use is essential not only for cost reduction but also for ensuring environmental sustainability and safeguarding human health. However, in many production systems, pesticide application remains highly inefficient. Globally, annual pesticide consumption exceeds 3 million tonnes, with approximately 45% used in the European Union and 25% in the United States (Sharma *et al.*, 2019). In Türkiye, the estimated annual requirement is around 15,000 tonnes, yet actual usage surpasses 40,000 tonnes. This substantial discrepancy is largely due to outdated spraying equipment and the absence of precision application technologies, leading to environmental contamination, groundwater pollution, and occupational health risks. Additionally, wind drift frequently disperses pesticides to non-target areas, further reducing application efficiency. To address these challenges, significant progress has been made in precision agriculture, with a strong focus on optimizing pesticide delivery while minimizing waste. Intelligent sprayers equipped with GPS-guided variable-rate control and solenoid valve regulation enable site-specific application, reducing unnecessary spraying and lowering off-target deposition. When combined with orchard maps, computer-controlled nozzles, and image-based canopy analysis, such systems have been shown to cut chemical inputs by 50-60% (Cross *et al.*, 2003; Da Silva *et al.*, 2006; Duga *et al.*, 2015). Furthermore, emerging innovations such as electrostatically charged spraying systems that enhance droplet adhesion to foliage, and autonomous electric platforms that eliminate fossil fuel dependency offer additional opportunities for cost savings and environmental protection.

Leveraging these technological developments, autonomous agricultural robots are increasingly recognized as a comprehensive solution for achieving both precision and sustainability in orchard management. These platforms integrate image processing, machine learning, and neural networks to optimize navigation and deliver highly targeted spraying. As highlighted by (Ünal, 2020), while such robots have the potential to replace conventional tractors in certain operations, they require exceptionally reliable navigation systems for tasks such as planting, spraying, and harvesting. Yet, studies have shown that conventional GPS and compass systems, such as the Honeywell HMR3000 and Topcon RTK GPS, can exhibit limitations in angular data accuracy.

To address these constraints, researchers have developed advanced navigation strategies such as SLAM-based mapping, sensor fusion, and image-guided obstacle detection which have shown promising results in orchard environments. Kıvanç *et al*. (2019) designed an unmanned ground vehicle that integrates mapping, localization, and obstacle detection via a hybrid filter for low-precision GPS, utilizing SLAM and Hector algorithms for both indoor and outdoor navigation. Similarly, Stefas *et al*. (2019) implemented image-based obstacle detection in apple orchards to counteract GPS unreliability near ground level. (Gerdan Koc and Vatandas, 2025) developed an autonomous fruit transportation robot equipped with a hybrid navigation system based on the robot operating system (ROS). The platform integrated LiDAR, an inertial measurement unit (IMU), and wheel encoders to enhance localization accuracy, and was successfully tested across different terrain conditions. Han *et al*. (2020) proposed a CNN-based path detection method for orange orchards during spraying, whereas (Gao *et al*., 2020) achieved 97.5% accuracy in peach orchard path planning using a color–depth data fusion technique.

Building on these advancements, the present study introduces an autonomous, electrostatically charged orchard spraying robot designed for both remote and fully autonomous operation. The system can be accessed from any location via mobile applications (Android, iOS, Windows) on smartphones and tablets. Field trials were conducted in the orchards of the Ankara University Faculty of Agriculture to evaluate operational efficiency, precision in pesticide application, and adaptability to varying orchard conditions. Unlike previous studies, this work integrates an electrostatically charged variable-rate spraying system with real-time AI-based canopy detection on a fully autonomous electric orchard robot. This combination enables selective, high-coverage pesticide application with reduced chemical usage, representing a novel and sustainable approach to orchard management. This study presents the first integration of electrostatic variable-rate spraying with real-time AI canopy detection on a fully autonomous electric platform, addressing a critical gap in precision orchard robotics.

Materials and Methods

Mechanical design

OrcBOT is a four-wheeled, fully electric mobile platform designed for precision and targeted spraying in orchards. The platform measures 2000 × 1100 × 850 mm (L × W × H) and is built on a chassis fabricated from 40 × 60 × 2.5 mm rectangular steel profiles, with the body assembled from 20 × 20 × 1.2 mm box profiles. The load-bearing structure was welded via gas metal arc welding (MIG/MAG) to ensure durability in orchard conditions (Figure 1). The front axle adopts a swing design, and the rear axle is driven by a differential powered by a 1600 W DC motor at 60 V. Steering is provided by a 24 V, 500 W DC motor coupled with an independent front axle to improve maneuverability. A hydraulically adjustable three-point hitch allows vertical (Z-axis) adjustment to accommodate different crop heights. The chassis is enclosed by molded fiberglass panels and equipped with operational safety features including signal lights, LED headlights, an overhead safety lamp, and a reverse warning buzzer. The assembled platform with mechanical components is shown in Figure 2.

Electronic and navigation systems

The navigation system integrates a centimeter-level RTK-GPS kit (simpleRTK2B), a Pixhawk PX4 2.4.8 flight controller, telemetry modules, SD card data logging, Bluetooth modules, and antennas. Mission routes were generated in Mission Planner software using Google Maps coordinates and uploaded to the Pixhawk via telemetry (Figure 3). A 360° LiDAR sensor supports obstacle avoidance, with data processed in real time using the Hector SLAM algorithm within a ROS framework. OrcBOT can operate in either autonomous or manual mode, with the latter controlled via an Android-based Bluetooth application and an Arduino Nano motor driver. In autonomous mode, PWM signals from the Pixhawk are sent directly to the motor drivers to provide full control. In this study, bidirectional communication between the Pixhawk 2.4.8 control unit and a ROS1-based onboard computer was established through the MAVLink protocol to enable autonomous driving of the ground vehicle. While the ArduRover

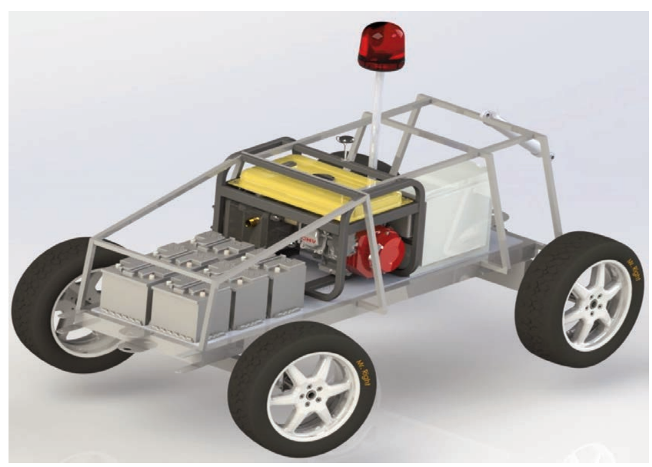

Figure 1. General view of OrcBOT.

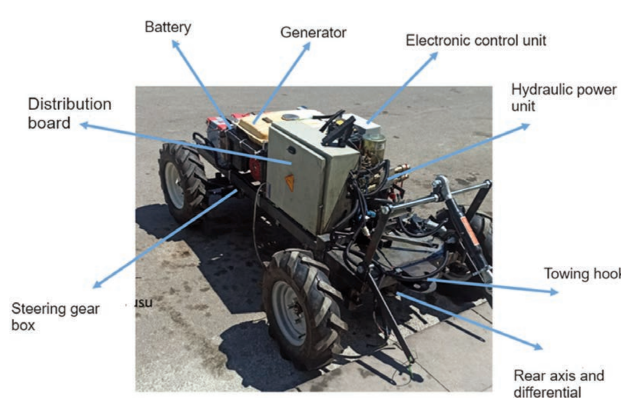

Figure 2. OrcBOT mechanical components view.

firmware running on the Pixhawk handled low-level speed and steering control, advanced perception and path-planning processes were executed within the ROS1 environment. LiDAR, IMU, and GNSS data were fused in ROS to continuously update the vehicle's position and surrounding conditions, and the generated velocity and steering commands were transmitted to the Pixhawk *via* the MAVROS interface. The Pixhawk processed these commands and produced the required motor driver signals, allowing the system to autonomously follow the designated route. Through this architecture, a stable, safe, and real-time autonomous driving performance was achieved.

AI-assisted variable-rate spraying unit

The spraying system consists of three 1.0, 1.2 and 1.5 mm (TeeJet hollow-cone nozzles, a high-pressure 12 V DC pump, and an adjustable electrostatic charging unit (0-20 kV) operating *via* the corona method (Table 1). Electrostatic spraying charges droplets at the nozzle tip, improving deposition, especially on the undersides of leaves. The unit is powered by a high-voltage transformer and regulated through a PWM-based circuit. The artificial intelligence-based tree recognition process, including both algorithmic detection and robotic spraying operation, is illustrated in Figure 4.

Canopy detection system

Canopy detection employed an Intel RealSense D435 depth camera to capture synchronized RGB and depth images at 1280 × 720 resolution. This reduced false positives from non-foliage elements and enabled accurate canopy segmentation. Detection used a YOLOv5 object detection model trained on approximately 400 annotated apple tree images collected under varying light and weather conditions. The YOLOv5s model was trained using SGD optimizer (lr=0.01, momentum=0.937) for 100 epochs. Data split: 70% train, 15% validation, 15% test. Training was performed in PyTorch with standard data augmentation techniques, and the model was deployed to an Nvidia Jetson Xavier NX for real-time inference. Upon canopy detection, the control unit triggered the spraying system, enabling variable-rate application in canopy zones only.

System integration and power management

The spraying unit was synchronized with RTK-GPS-based autonomous navigation for precise application. GPS data and wheel encoder readings were processed by the control algorithm to adjust spray timing and duration. The autonomous driving schematic diagram is given in Figure 5. Power was supplied by a 60 V battery pack, with 5 V and 12 V outputs provided by DC–DC converters for sensors and controllers. Steering was actuated by an electric actuator with positional feedback, calibrated via a laser distance sensor (Figure 6). The Pixhawk 2.4.8 served as the central navigation module, with route planning, sensor calibration, GPS monitoring, and log data management carried out in Mission Planner. Figure 7 displays the RC controls and designated task buttons. In autonomous mode, the vehicle cannot be controlled remotely. Only the transition signal to autonomous mode is conveyed via mode adjustment. Table 2 also includes the electronic hardware components.

Experimental design and orchard trials

Field experiments were conducted in the orchards of the Ankara University Faculty of Agriculture and were organized into two main groups. In the first group, apple, pear, and quince orchards representing different fruit types were utilized to assess route planning and determine the robot's route calibration accuracy. In the second group, the spraying performance of the robot and the artificial intelligence-based detection processes were evaluated. Within this scope, the detection performance of the YOLOv5 model used for canopy identification was examined exclusively through trials conducted in the apple orchard. The precision, recall, and mean average precision (mAP) values of the YOLOv5 algorithm were calculated to demonstrate its real-time detection capability. Additionally, the spraying performance of the robot was

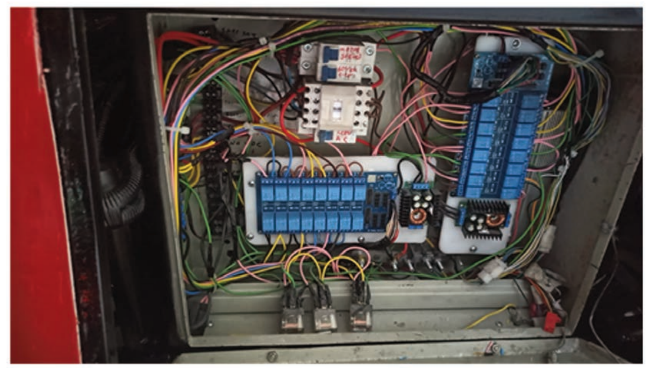

Figure 3. OrcBOT electrical panel.

Figure 4. Artificial intelligence-based tree recognition. **a**) Artificial intelligence application. **b**) Operation of the robotic spraying mechanism.

Table 1. Pump characteristics.

Parameter name	Value
Liquid transport capacity	5.1 L/min
Maximum pressure	100 PSI (7 bar)
Current	4.5 Amper
Voltage	12 Volt DC
Hose size	10 mm

assessed based on key parameters such as target surface coverage, spray uniformity, droplet density, and droplet distribution uniformity, with these metrics derived from application tests performed in the apple orchard. The trials were carried out in an apple orchard with tree rows spaced 3 m apart and tree heights ranging from 1.5 to 2.5 m. These experimental conditions provided a consistent and controlled environment for evaluating both the navigation performance and spraying efficiency of the autonomous system.

The experimental design included three travel speeds (1, 3, and 5 km/h), three electrostatic voltages (10, 15, and 20 kV), and three spray pressures (2, 4, and 6 bar), arranged in a factorial layout with three replications (Table 3). A food dye–water mixture was used as the spray solution to facilitate droplet visualization.

The autonomous vehicle was equipped with an RTK-GPS module, IMU, 360° LIDAR sensor, stereo cameras, a Pixhawk 2.4.8 flight controller, Arduino Mega 2560 microcontrollers, onboard processors, and dedicated control software. Motor speed was regulated *via* pulse width modulation (PWM), ensuring a proportional relationship between pulse duration and wheel rotation speed. Autonomous navigation was managed using Mission Planner software, where waypoint-based routes were generated from Google Maps and uploaded to the Pixhawk via telemetry.

Spraying performance was evaluated using 7.16 cm^2 water-sensitive papers (Syngenta) placed at the upper, middle, and lower

Table 2. Electronic components and their specifications.

Component	Task on the vehicle
Pixhawk 2.4.8	Acts as the flight controller of the vehicle, processing data from GPS and other sensors to ensure the stabilization of the agricultural vehicle and can be programmed for automatic driving tasks.
Arduino Mega	Processes signals from Pixhawk according to the generated algorithm and sends digital signals to relays.
72V 1500W DC motor speed controller	Electronic devices used to control and operate the vehicle's electric motor.
12V 60Ah battery	Provides power to the electronic systems on the vehicle.
SimpleRTK2B – Starter Kit LR GPS	GPS (Global Positioning System) assists autonomous vehicles in determining accurate positioning.
Pixhawk telemetry 500mW	Enables communication between the ground station (base) and the vehicle.
RC controller receiver 9 channel	Triggers the relays in control mode.
Voltage regulator 5V	Reduces the voltage from the battery to 5 volts.
Relay 16 channel	Allows current reversal when needed.
Linear motor	Enables steering of the vehicle.
VL53L0X Laser	Measures steering angle and communicates it to Pixhawk.

Table 3. Experimental design.

Pressure (bar)	Nozzle diameter (mm)	Electrostatic (kV)	Forward speed (km/h)
2-4-6	IDK-AD 90 (1.0, 1.2, 1.5)	10-15-20	1-3-5

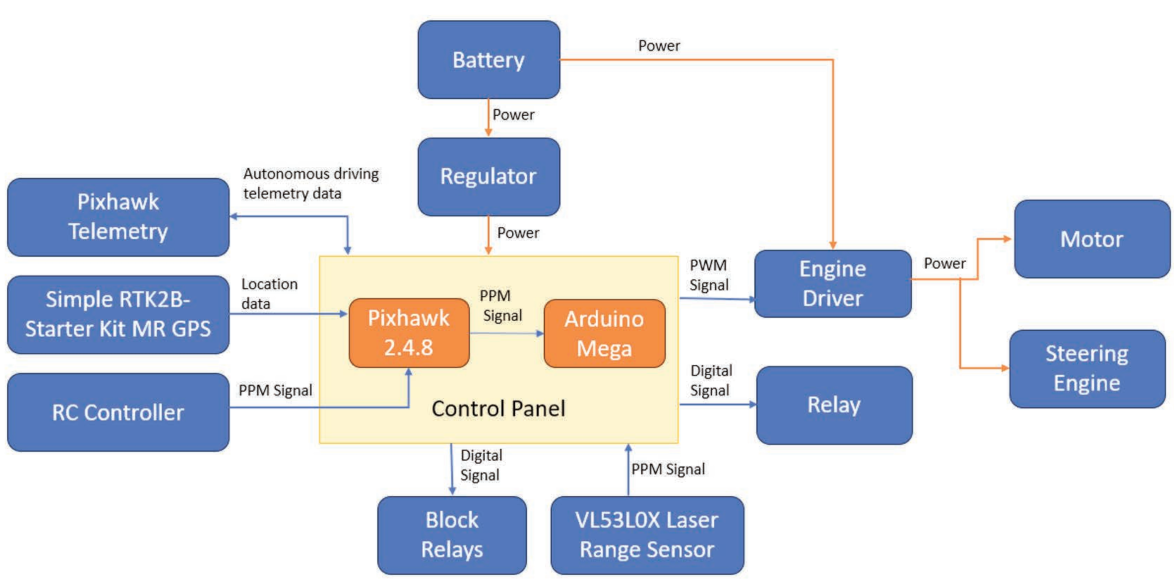

Figure 5. Autonomous driving schematic diagram.

canopy levels of apple trees. The vehicle was fitted with TeeJet hollow-cone nozzles (0.8 mm) operating at 7 bar pressure and a travel speed of 3.6 km/h. After spraying, cards were collected and analyzed according to the method of Çilingir and Dursun (2010) for volume median diameter (VMD) calculation. Image analysis was performed in ImageJ by scanning the cards, converting them to 8-bit grayscale, and applying particle analysis to determine droplet size distribution and canopy coverage percentage.

Results

Evaluation of the AI model

The study tested the tree canopy detection model, trained for orchard trials, using an object detection algorithm. The canopy detection algorithm encapsulates identified target objects within square frames, displaying the detection and prediction rates of each frame as percentage labels on the screen. The mean average precision (mAP) graph indicates successful performance, surpassing a confidence threshold of 0.5 after 90 training iterations. The precision-confidence curve of the model utilizing the YOLOv5 algorithm achieved near-perfect performance in detecting tree canopies at a confidence level of 0.827.

The YOLOv5 algorithm employed for artificial intelligence-driven canopy detection and spraying has demonstrated marginally reduced efficacy relative to existing literature. In neural network studies, augmenting the quantity of trained samples is essential for enhancing success rates. The limited quantity of labeled data samples relative to existing literature is a crucial factor influencing the diminished success rate. Nonetheless, the materials, methods, and techniques employed in the trials proved effective. Plans have been established post-project to enhance the success rate. A contributing factor to the diminished success rate in artificial intelligence trials may be the limited capacity of the Jetson Xavier board.

Evaluation of orchard spraying performance

The analyses performed using the Image J program yielded calculations of average droplet diameter and coverage ratios (Table 4). Conclusions regarding spraying performance have been drawn by comparing parameters such as the number of droplets, the area covered by the droplets, and the coverage ratio on Syngenta brand water-sensitive papers. During the spraying process, 2852 droplets were observed at the bottom point, 2325 droplets at the middle point, and 2122 droplets at the top point. The measured average droplet diameters were 152 µm, 167 µm, and 154 µm, respectively. The extent of the droplet coverage and the corresponding ratios are also included. The coverage ratios were determined to be 54.46%

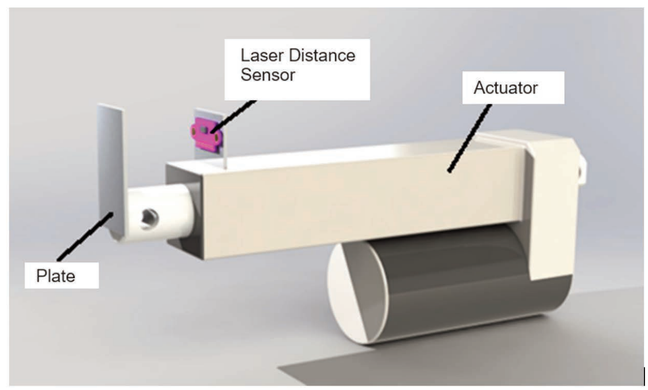

Figure 6. Steering system view.

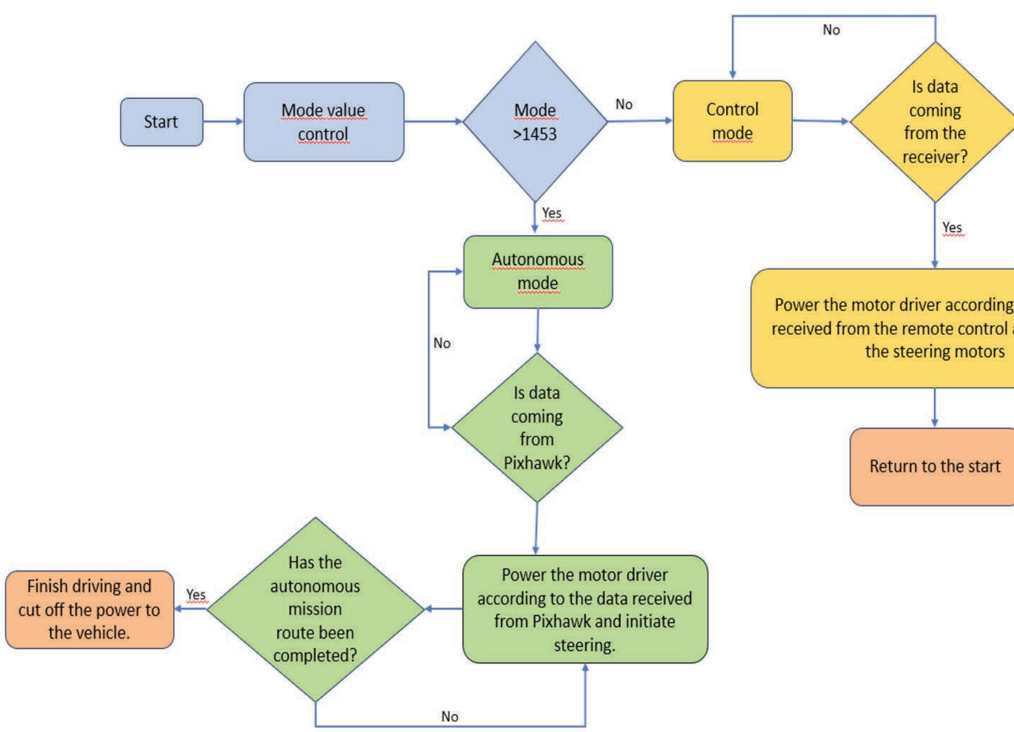

Figure 7. Flow diagram of autonomous vehicle RC control.

at the lowest point, 57.84% at the midpoint, and 52.36% at the highest point. Consequently, to ascertain the success criteria of the precision spraying system, a map with GPS coordinates and marker paths was created in the orchard. To simulate spraying, a mixture of food dyes and water was applied to apple trees in the experimental orchard, where water-sensitive papers were positioned at three distinct heights. The experimental layout consisted of three levels of speed factor, three levels of operating height factor, and randomized plots arranged in factorial order. The values recorded from the water-sensitive papers during the experiments were analyzed using the SPSS software, and ANOVA was employed to assess any deviations from the target areas in the spraying conducted across the three designated sections. The results obtained are displayed in Table 5. ANOVA results revealed that coverage ratio was significantly influenced by repeat position, pressure, nozzle diameter, electrostatic voltage, and travel speed (p<0.05), while droplet diameter was significantly affected by all factors except electrostatic voltage (p>0.05). Across canopy levels, coverage ratios were 54.46% at the lower position, 57.84% at the middle, and 52.36% at the upper canopy, with corresponding droplet diameters of 152 µm, 167 µm, and 154 µm, respectively. Pressure exerted the strongest effect on droplet size and coverage: spraying at 2 bar achieved the highest coverage (~57%) and largest droplets (~231 µm), whereas 6 bar resulted in the lowest coverage (~52%) and smallest droplets (~163 µm). Increasing nozzle diameter from 1.0 to 1.5 mm slightly improved coverage but also increased droplet size from ~177 µm to ~202 µm. The optimal electrostatic voltage for coverage was 10 kV (~57%), with higher voltages (15-20 kV) providing no significant improvement.

Travel speed showed a clear negative relationship with coverage ratio and droplet size: 1 km/h yielded ~57% coverage with 216 µm droplets, whereas 5 km/h reduced coverage to ~52.5% and droplet size to ~187 µm. Overall, these results indicate that moderate pressure (2 bar), lower travel speed (1 km/h), and 10 kV electrostatic voltage provided the best combination of canopy coverage and droplet characteristics under the tested orchard conditions. The calculated spraying rates of OrcBOT under different speed, nozzle diameter, and pressure conditions are presented in Table 6.

Table 4. Average droplet diameter and coverage ratios obtained in the experiments.

Water-sensitive card location	Droplet count	Average droplet diameter (µm)	Coverage ratio (%)
Bottom point	2852	152	54.46
Middle point	2325	167	57.84
Top point	2122	154	52.36

Droplet sizes (150-170 µm) fall within the optimal range for insecticide penetration.

Table 5. Analysis of variance.

Factor	Level	n	Coverage ratio (%)	Droplet diameter (µm)
Repeat	Bottom	60	54.46±0.99^{A}**	152±6.44^{A}*
	Middle	60	57.84±1.24^{AB}	167±8.43^{AB}
	Top	60	52.36±1.13^{B}	154±8.08^{B}
Pressure (bar)	2	54	57.00±1.18^{A}**	231.48±9.33^{A}**
	4	60	55.00±1.29^{A}	191.25±7.02^{B}
	6	66	52.00±0.78^{B}	162.90±4.43^{C}
Nozzle diameter (mm)	1.0	54	54.00±0.94^{A}*	176.88±3.27^{A}**
	1.2	72	55.00±1.08^{AB}	197.89±5.87^{B}
	1.5	54	57.00±1.34^{B}	202.30±12.10^{C}
Electrostatic voltage (kV)	10	54	57.00±1.14^{A}**	196.67±9.06 ns
	15	72	54.00±1.01^{B}	186.97±5.97
	20	54	54.50±1.22^{B}	195.09±8.88
Speed (km/h)	1	54	57.00±1.41^{A}**	215.50±11.70^{A}**
	3	72	55.00±1.01^{AB}	180.67±4.38^{B}
	5	54	52.50±0.88^{B}	186.66±6.50^{C}
General mean	–	180	55.00±0.66	192.92±4.48

Values are means ±SE. $^{A-C}$Significant differences according to Tukey's test; *p<0.05, **p<0.01, ns, not significant.

Table 6. Calculation of OrcBOT's spraying rate.

Speed (km/h)	Nozzle diameter (mm)	Pressure (bar)	Orifice area (m^2)	Flow rate (L/min)
1	1	2	0.00000079	0.105333333
3	1,2	4	1,1376E-06	0.45504
5	1,5	6	1,7775E-06	1.185

Discussion

The autonomous navigation trials demonstrated consistent route-following performance, with the vehicle successfully reaching designated waypoints along linear paths. Deviations of up to approximately 1 m were observed during turning maneuvers, primarily due to horizontal dilution of precision (HDOP) variability and local multipath effects in the orchard. While this error margin is acceptable for non-critical navigation tasks, it is greater than the lateral deviations reported in recent LiDAR-integrated orchard robots, which have achieved RMSE values of 11.4-15.5 cm and lateral errors under 22 cm (Jiang and Ahamed, 2023; Liu *et al*., 2022). This difference is largely attributable to the absence of multi-sensor fusion (LiDAR, IMU, wheel encoders) and advanced trajectory correction algorithms such as Extended Kalman Filtering (Su *et al*., 2024) or point cloud-based SLAM (Jiang and Ahamed, 2023). Integrating such methods could reduce reliance on GPS-only positioning, especially in GNSS-obstructed conditions caused by dense canopies or nearby structures.

Steering performance was another factor influencing navigation accuracy. The initial 1000 N and 2000 N DC actuators exhibited steering delays of 5-7 s under load, reducing maneuverability in tight orchard turns. The upgraded 6000 N actuator, calibrated via a VL53L0X laser sensor with a 35 mm neutral stroke point, markedly improved responsiveness. Compared with alternative architectures such as four-wheel independent steering or articulated designs (Lakkad, 2004.), the actuator-driven front axle system offers a practical balance between mechanical simplicity, energy efficiency, and turning capability. Nevertheless, additional precision could be achieved through closed-loop positional feedback control.

Table 7 provides a comparative analysis of autonomous orchard spraying systems in the literature, focusing on technical methodology, sensor configuration, control systems, and orchard type. LiDAR-based navigation is common in many studies (Jiang and Ahamed, 2023; Liu et al., 2022), offering reliable spatial mapping but generally requiring higher investment and computational capacity. In contrast, vision-based methods, such as those in Lippi *et al*. (2024) and the present study, reduce hardware costs while leveraging deep learning for canopy-related applications. Many autonomous sprayers adopt PID or ROS-based control frameworks (Liu *et al*., 2022; Partel *et al*., 2021a); whereas others integrate AI modules for dynamic decision-making (Akdoğan *et al*., 2024; Luo Y *et al*., 2025). The Pixhawk-Jetson Xavier configuration used here enables concurrent navigation and electrostatic spray control -a combination less frequently reported in previous works.

The reviewed studies encompass orchard types including citrus, hazelnut, apple, and cherry, whereas this study focuses on apple orchards, characterized by distinct canopy geometries and leaf surface properties that influence spray deposition. By incorporating electrostatics into the spraying process, the system addresses challenges related to droplet adherence and canopy penetration, providing a distinct operational advantage over most platforms examined in comparable research.

The YOLOv5-based canopy detection model achieved an mAP@0.5 above 0.5, precision of 0.827, and an F1-score of 0.95 after 90 training iterations, indicating reliable canopy recognition in orchard environments. Precision values were slightly lower than those in UAV-based spraying (98-98.6%; Akdoğan *et al*., 2024) and multi-robot YOLOv8 systems (95%). The reduced precision is likely due to the limited size and diversity of the annotated training dataset and the computational constraints of the NVIDIA Jetson Xavier platform, which restrict real-time inference throughput. Literature consistently demonstrates that dataset expansion including varied lighting conditions, seasonal canopy differences, and occlusions improves detection robustness (Chen *et al*., 2024; Koirala *et al*., 2019). Planned improvements include dataset augmentation and hardware upgrades to approach benchmark performance.

Field spraying trials yielded mean droplet diameters of 152 μm, 167 μm, and 154 μm for lower, middle, and upper canopy levels, respectively, with corresponding coverage ratios of 54.46%, 57.84%, and 52.36%. These results match fine spray classification (ASAE S572.1) and are consistent with the 50-60% coverage range reported for precision spraying systems (Chen *et al*., 2022; Gil *et al*., 2014). ANOVA indicated that coverage ratio was significantly influenced by spray pressure, nozzle diameter, electrostatic voltage, and travel speed ($p<0.05$), while droplet size was affected by all factors except electrostatic voltage ($p>0.05$). Optimal coverage (~57%) and droplet size (~231 μm) occurred at 2 bar pressure, 1 km/h travel speed, and 10 kV electrostatic voltage, aligning with the 10-12 kV range reported as optimal for uniform charge distribution (Yamane and Miyazaki, 2017; Zhang *et al*., 2010).

Electrostatic spraying efficiency declined under high humidity, attributed to conductive moisture accumulation on the metallic chassis, which caused premature charge dissipation. This aligns with earlier findings (Appah *et al*., 2019), highlighting the need for chassis insulation and hydrophobic coatings to maintain consistent performance. Comparable studies have reported reductions in non-target coverage (49.72%) and spray volume (~49%) when using intelligent sprayers (Seol *et al*., 2022). Across the literature, chemical usage reductions from 19.19% to 74% have been documented (Yu *et al*., 2025), with the present system's performance falling within the mid-to-upper range of these values.

Beyond technical performance, the electric drive system offers operational and environmental benefits. The robot's 5-hour endurance per charge, at an energy cost of approximately USD 0.76, contrasts sharply with the ~15 L diesel consumption (≈USD 19.70) of a 55 hp tractor over the same period -representing over 95% reduction in fuel cost. Furthermore, the absence of exhaust emissions supports compliance with emerging low-emission agricultural policies and enhances operator safety in enclosed orchard environments. These sustainability gains, combined with competitive coverage rates and AI-assisted targeting, position the developed platform as a viable solution for precision, low-impact orchard crop protection.

Conclusions

The autonomous pesticide spraying robot, built at approximately half the size of a conventional tractor, operates electrically with generator support and can reach speeds of up to 30 km/h when unladen. Equipped with hydraulic units, towing hooks, and multiple power outputs (12V, 24V, 220V), it accommodates a variety of agricultural implements. The system supports both autonomous and remote-controlled operation, managed through embedded software (Pixhawk, Arduino Mega) and integrating YOLOv5-based AI for real-time canopy detection and targeted spraying. The electrostatic spraying unit, using the corona method, delivers up to 20 kV to enhance droplet adhesion and uniform coverage.

This study presents one of the first integration of an electrostatically charged variable-rate spraying mechanism with real-time AI-driven canopy detection on a fully autonomous electric orchard

Table 7. A comparative analysis of control systems, sensing components, and application contexts in studies of autonomous orchard spraying.

Study	Technical approach	Sensor types	Control system	Application context
Our study (2025)	AI-driven canopy detection and precision electrostatic spraying	Machine vision camera, RTK-GPS, LiDAR	Pixhawk flight controller, Jetson Xavier, RTK-GPS navigation, electrostatic spray control	Apple orchard
Jiang and Ahamed, 2023	LiDAR-based navigation, DBSCAN/K-means/RANSAC, PID	LiDAR	Incremental PID steering, Arduino relay	Artificial tree-based orchard, concrete, grass; GNSS obstruction
Liu *et al.*, 2022	3D LiDAR, RANSAC, Euclidean clustering	3D LiDAR, encoder, IMU	PID, ROS	Modernized pear plantation
Partel *et al.*, 2021a	Sensor fusion, AI (CNN)	LiDAR, RGB camera, GPS, flow meters	Sensor fusion, AI, C++	Citrus orchard
Lippi *et al.*, 2023	YOLO-based detection, 3D reconstruction	RGB-D camera	YOLO, Kimera, ROS	Hazelnut orchard
Akdoğan *et al.*, 2024	AI-based UAV, YOLOv5/7/8	Machine vision cameras	AI-integrated, YOLO	Cherry trees
Mu *et al.*, 2023	Cartesian robot, mask R-CNN	Stereo camera (ZED2)	Machine vision, cartesian robot	Apple orchard, trellis-trained
Partel *et al.*, 2021b	Sensor fusion, YOLOv3	RGB cameras, 2D LiDAR, GPS	Electronic valve, AI	Citrus orchard
Mu *et al.*, 2024	UGV, machine vision	Machine vision cameras	No mention found	Apple orchard
Luo *et al.*, 2025	Machine vision, fuzzy adaptive control	Machine vision cameras	Fuzzy adaptive, ESO, GrabCut	Artificial and natural orchards
Costa and Ampatzidis, 2022	Sensor fusion, CNN	LiDAR, machine vision, GPS, flow meters	Integrated sensor-actuator	Citrus orchard
Moorehead *et al.*, 2012	Multi-tractor, radar, cameras	LiDAR, cameras	Geometric/appearance-based	Citrus orchard, cluttered
Jiang *et al.*, 2024	3D LiDAR SLAM, NDT_ICP	3D LiDAR	ROS, NDT_ICP	Peach orchard, GNSS obstruction
Tekin and Demir, 2025	UAV, color-based detection	GPS, IMU, stereo camera	Pixhawk, Mission Planner	Artificial orchard, grass, weather
Wang *et al.*, 2022	3D LiDAR, radar, ADRC	3D LiDAR, radar, ultrasonic	ADRC, PID, ROS	Orchard, complex canopy
Chen et al., 2021	Drone, Tiny-YOLOv3	Camera	YOLOv3, NVIDIA TX2	Longan orchard
Vu *et al.*, 2024	Stereo vision, sensor fusion, DWA	Stereo cameras, RTK-GNSS, IMU	ROS2, DWA	Fruit orchards, signal instability
Kim *et al.*, 2020	SegNet, semantic segmentation	RGB-D camera	CNN (SegNet)	Pear orchard
Cho and Ki	Fuzzy logic, machine vision	Machine vision, ultrasonic	Fuzzy Logic Controller (FLC)	Orchard, obstacles
Deguchi *et al.*, 2023	AI-based grape detection	Vision (not specified)	Deep learning	Vineyard
Han *et al.*, 2021	GNSS, sensor fusion, EKF	GNSS, motion sensors	EKF, vehicle control	Apple orchard
Ren *et al.*, 2022	Double DQN, virtual radar	XN422 navigation system	Double DQN, Python/TensorFlow	Persimmon orchard, GNSS drift
Oberti *et al.*, 2013	Modular robot, multispectral	Multispectral camera	Optical feedback	Vineyard, greenhouse
Kim *et al.*, 'Preliminary experimental results'	SegNet, semantic segmentation	Camera	CNN (SegNet)	Pear orchard
Oberti *et al.*, 2016	Modular robot, multispectral	Multispectral (R-G-NIR) camera	Optical feedback	Vineyard, greenhouse
Shrinidhi *et al.*, 2023	UAV, SLAM, YOLOv4	GPS, camera	PX4, LVQ, K-Means	Palm plantations
Yu et al., 2025	Swing-arm sprayer, photoelectric	Photoelectric sensor	Arduino, sensor delay compensation	Pear orchard, Beijing
Mahmud *et al.*, 2021	Airblast, LiDAR, fuzzy logic	LiDAR	Micro-controller, fuzzy logic	Apple orchard, dense canopy
He *et al.*, 2015	Tractor-mounted IR, electrostatics	Infrared sensor	IR detection, electrostatics	Chinese orchard
Osterman and Hočevar, 2014	Adaptive arms, 2D LiDAR	2D LiDAR	LabVIEW, modular	Orchard
Seol *et al.*, 2022	Real-time flow, SegNet	RGB-D cameras	PWM, solenoid valves	Pear orchard, unstructured roads
He and Salyani, 2011	Tractor-mounted IR, electrostatics	Infrared sensor	Electromagnetic valve, high voltage	Apple orchard, dense canopy
Berk *et al.*, 2019	Fuzzy logic, ultrasonic	Ultrasonic sensors	Fuzzy logic, Matlab/Simulink	Artificial orchard
Gao *et al.*, 2019	UAV, MSM, ML	4K camera	MSM, MATLAB	Croplands, orchards

robot. This combination enables selective, high-coverage pesticide application while reducing chemical usage by 49-72% ($p<0.05$; Table 5) and off-target deposition. Field validation confirmed 57% canopy coverage and 152-167 µm droplet size under optimal parameters (2 bar, 1 km/h, 10 kV), positioning OrcBOT as a sustainable solution for precision agriculture. In addition to improving environmental sustainability, the system offers 95% lower operating costs ($0.76 *vs* $19.70/5h) and reduces fossil fuel dependency. Current limitations include navigation drift during sharp turns (~1 m error) and reduced AI accuracy under dense canopies (82.7% precision), necessitating future integration of multi-sensor fusion. Its modular design provides a flexible foundation for scaling to diverse orchard types and operational conditions.

References

Akdoğan C, Özer T, Oğuz Y, 2024. Design and implementation of an AI-controlled spraying drone for agricultural applications using advanced image preprocessing techniques. Robot Intell Autom 44:131-151.

Appah S, Wang P, Ou M, Gong C, Jia W, 2019. Review of electrostatic system parameters, charged droplets characteristics and substrate impact behavior from pesticides spraying. Int J Agric Biol Eng 12:1-9.

Chen CJ, Huang YY, Li,YS, Chen YC, Chang CY, Huang YM, 2021. Identification of fruit tree pests with deep learning on embedded drone to achieve accurate pesticide spraying. IEEE Access 9:21986-21997.

Chen P, Xu W, Zhan Y, Wang G, Yang W, Lan Y,. 2022. Determining application volume of unmanned aerial spraying systems for cotton defoliation using remote sensing images. Comput Electron Agric 196:106912.

Chen Y, Liu Z, Lin Z, Xu Z, Guan X, Zhou Z, et al., 2024. UAV-UGV cooperative targeted spraying system for honey pomelo orchard. Int J Agric Biol Eng 17:22-31.

Cho S, Ki N, 1999. Autonomous speed sprayer guidance using machine vision and fuzzy logic. T ASAE 42:1137-1143.

Çilingir I, Dursun E, 2010. [Crop protection machinery].[Article in Turkish]. Ankara University Faculty of Agriculture Publications 1531.

Costa L, Ampatzidis Y, 2022. Smart tree crop sprayer sensing system utilizing sensor fusion and artificial intelligence. Proc. 2022 ASABE Annual Int. Meet.

Cross JV, Walklate PJ, Murray RA, Richardson GM, 2003. Spray deposits and losses in different sized apple trees from an axial fan orchard sprayer: 3. Effects of air volumetric flow rate. Crop Prot 22:381-394.

Da Silva A, Sinfort C, Tinet C, Pierrat D, Huberson S, 2006. A Lagrangian model for spray behaviour within vine canopies. J Aerosol Sci 37:658-674.

Deguchi T, Baltazar AR, dos Santos FN, Mendonça H, 2023. Vision-based smart sprayer for precision farming. Proc. Iberian Robotics Conf.

Duga AT, Ruysen K, Dekeyser D, Nuyttens D, Bylemans D, Nicolai BM, 2015. Spray deposition profiles in pome fruit trees: Effects of sprayer design, training system and tree canopy characteristics. Crop Prot 67:200-213.

Gao G, Ke X, Yu CJ, 2020. A spraying path planning algorithm based on colour-depth fusion segmentation in peach orchards. Comput Electron Agr 173:105412.

Gerdan Koc D, Vatandas M, 2025. Development and performance analysis of an autonomous agricultural vehicle for fruit transportation. J Field Robot 42:3189-3212.

Gil E, Balsari P, Gallart M, Llorens J, Marucco P, Andersen PG, et al., 2014. Determination of drift potential of different flat fan nozzles on a boom sprayer using a test bench. Crop Prot 56:58-68.

Han JH, Park CH, Jang YY, Gu JD, Kim CY, 2021. Performance evaluation of an autonomously driven agricultural vehicle in an orchard environment. Sensors (Basel) 22:114.

Han SH, Kang KM, Hwang RY, Choi CH, Lee DH, 2020. Deep learning-based path detection in citrus orchard. Proc. ASABE Ann. Int. Virtual Meet. St. Joseph: 2000287.

He X, Yang F, Qiu B, 2024. Agricultural environment and intelligent plant protection equipment. Agronomy 14:937.

He X, Zeng A, Liu Y, Song J, 2011. Precision orchard sprayer based on automatically infrared target detecting and electrostatic spraying techniques. Int J Agric Biol Eng 4:35.

Jiang A, Ahamed T, 2023. Navigation of an autonomous spraying robot for orchard operations using LiDAR for tree trunk detection. Sensors (Basel) 23:4808.

Jiang S, Qi P, Han L, Liu L, Li Y, Huang Z, et al., 2024. Navigation system for orchard spraying robot based on 3D LiDAR SLAM with NDT_ICP point cloud registration. Comput Electron Agr 220:108870.

Kim J, Seol J, Lee S, Hong SW, Son HI, 2020. An intelligent spraying system with deep learning-based semantic segmentation of fruit trees in orchards. Proc. IEEE Int. Conf. on Robotics and Automation (ICRA), Paris; pp. 3923-3929.

Kivanç ÖC, Mungan TE, Berkin A, Gürkan T, 2019. [An integrated approach to development of unmanned ground vehicle: Design, analysis, implementation and suggestions].[Article in Turkish]. J Fac Eng Archit Gaz 34:1957-1973.

Koirala A, Walsh KB, Wang Z, McCarthy C, 2019. Deep learning – Method overview and review of use for fruit detection and yield estimation. Comput Electron Agr 162:219-234.

Lakkad S, 2004. Modeling and simulation of steering systems for autonomous vehicles. Ph.D. Thesis, Florida State University.

Lippi M, Santilli M, Carpio RF, Maiolini J, Garone E, Cristofori V, Gasparri A, 2024. An autonomous spraying robot architecture for sucker management in large-scale hazelnut orchards. J Field Robot 41:2114-2132.

Liu L, Liu Y, He X, Liu W, 2022. Precision variable-rate spraying robot by using single 3D LIDAR in orchards. Agronomy 12:2509.

Luo Y, He X, Shi H, Yang SX, Song L, Li P, 2025. Design and development of a precision spraying control system for orchards based on machine vision detection. Sensors (Basel) 25:3799.

Mahmud MS, Zahid A, He L, Martin P, 2021. Opportunities and possibilities of developing an advanced precision spraying system for tree fruits. Sensors (Basel) 21:3262.

Moorehead SJ, Wellington CK, Gilmore BJ, Vallespi C, 2012. Automating orchards: A system of autonomous tractors for orchard maintenance. Available from: https://www.cs.cmu.edu/~cvalles/papers/automatingOrchards.pdf

Mu X, He L, Heinemann P, Schupp J, Karkee M, Zhu M, 2025. UGV-based precision spraying system for chemical apple blossom thinning on trellis trained canopies. J Field Robot 42:1000-1011.

Mu X, Hussain M, He L, Heinemann P, Schupp J, Karkee M, Zhu M, 2023. An advanced robotic system for precision chemical thinning of apple blossoms. J ASABE 66:1125-1134.

Oberti R, Marchi M, Tirelli P, Calcante A, Iriti M, Baur J, et al., 2013. Selective spraying of grapevine diseases by a modular agricultural robot. J Agr Eng 44:271.

Oberti R, Marchi M, Tirelli P, Calcante A, Iriti M, Hocevar M, Ulbrich H, 2014. The CROPS agricultural robot: application to selective spraying of grapevine's diseases. Proc. Int. Conf. Agricultural Engineering, Zurich: C0612.

Osterman A, Godeša T, Hočevar M, Stopar M, 2014. Fruit thinning with selective spraying. Proc. 42nd Int. Symp. Agricultural Engineering, Opatija; pp. 189-195.

Pan S, Ahamed T, 2022. Pear recognition in an orchard from 3D stereo camera datasets to develop a fruit picking mechanism using mask R-CNN. Sensors (Basel) 22:4187.

Partel V, Costa L, Ampatzidis Y, 2021a. Smart citrus tree sprayer utilizing sensor fusion and artificial intelligence. Proc. ASABE Annual Int. Virtual Meet, St. Joseph, American Society of Agricultural and Biological Engineers.

Partel V, Costa L, Ampatzidis Y, 2021b. Smart tree crop sprayer utilizing sensor fusion and artificial intelligence. Comput Electron Agr 191:106556.

Seol J, Kim J, Son HI, 2022. Field evaluations of a deep learning-based intelligent spraying robot with flow control for pear orchards. Precision Agric 23:712-732.

Sharma A, Kumar V, Shahzad B, Tanveer M, Sidhu GPS, Handa N, et al., 2019. Worldwide pesticide usage and its impacts on ecosystem. SN Appl Sci 1:1446.

Shrinidhi I, Pratham K, Ajith B, 2023. UAV platform for pesticide spraying and disease detection for areca nut and pepper plantations. Proc. IEEE Int. Conf. Distributed Computing, VLSI, Electrical Circuits and Robotics (DISCOVER), Mangalore; pp. 167-172.

Stefas N, Bayram H, Isler V, 2019. Vision-based monitoring of orchards with UAVs. Comput Electron Agr 163:104814.

Su Z, Zou W, Zhai C, Tan H, Yang S, Qin X, 2024. Design of an autonomous orchard navigation system based on multi-sensor fusion. Agronomy 14:2825.

Tekin AF, Demir BE, 2025. Autonomous agricultural spraying UAV: Design, implementation and performance analysis. Black Sea J Eng Sci 8:991-998.

Ünal I, 2020. [Determining the heading angle measurement accuracy of RTK GPS receiver by the help of digital compass].[Article in Turkish]. Mediterr Agric Sci 33:369-374.

United Nations, 2024. World Population Prospects 2024: Summary of Results. Available from: https://population.un.org/wpp/assets/Files/WPP2024_Summary-of-Results.pdf

Vu CT, Chen HC, Liu YC, 2024. Toward autonomous navigation for agriculture robots in orchard farming. Proc. IEEE Int. Conf. Recent Advances in Systems Science and Engineering (RASSE), Taichung; pp. 1-8.

Wang Y, Zhang Z, Jia W, Ou M, Dong X, Dai S, 2025. A review of environmental sensing technologies for targeted spraying in orchards. Horticulturae 11:551.

Yamane S, Miyazaki M, 2017. Study on electrostatic pesticide spraying system for low-concentration, high-volume applications. Jpn Agric Res Q 51:11-16.

Yu Z, Geng M, Zhao K, Meng X, Zhang H, He X, 2025. Design and experimental operation of a swing-arm orchard sprayer. Agronomy 15:1706.

Zhang Q, Liu J, Wang X, Li M, Yang J, 2010. Controlling internal nanostructures of porous microspheres prepared via electrospraying. Colloid Polym Sci 288:1385-1391.

Received: 8 March 2025; Accepted: 26 November 2025.

Contributions: all authors made a substantive intellectual contribution, read and approved the final version of the manuscript and agreed to be accountable for all aspects of the work.

Conflict of interest: the authors declare no competing interests, and all authors confirm accuracy.